

An antibiotic composite electrode for improving the sensitivity of electrochemically active biofilm biosensor

Shuyi Wang¹, Xiang Qi¹, Yong Jiang (✉)², Panpan Liu³, Wen Hao¹, Jinbin Han¹, Peng Liang (✉)¹

¹ State Key Joint Laboratory of Environment Simulation and Pollution Control, School of Environment, Tsinghua University, Beijing 100084, China

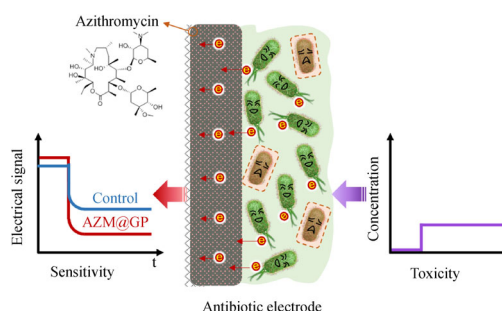
² Fujian Provincial Key Laboratory of Soil Environmental Health and Regulation, College of Resources and Environment, Fujian Agriculture and Forestry University, Fuzhou 350002, China

³ School of Ecology and Environment, Zhengzhou University, Zhengzhou 450001, China

HIGHLIGHTS

- Antibiotic azithromycin employed in graphite electrode for EAB biosensor.
- Azithromycin at 0.5% dosage increased the sensitivity for toxic formaldehyde.
- Azithromycin increased the relative abundance of *Geobacter*.
- Azithromycin regulated thickness of electroactive biofilm.

GRAPHIC ABSTRACT



ARTICLE INFO

Article history:

Received 25 August 2021

Revised 18 September 2021

Accepted 10 October 2021

Available online 3 December 2021

Keywords:

AZM@GP composite electrode

EAB-biosensor

Water quality early-warning

ABSTRACT

Extensive research has been carried out for improved sensitivity of electroactive biofilm-based sensor (EAB-sensor), which is recognized as a useful tool in water quality early-warning. Antibiotic that is employed widely to treat infection has been proved feasible in this study to regulate the EAB and to increase the EAB-biosensor's sensitivity. A novel composite electrode was prepared using azithromycin (AZM) and graphite powder (GP), namely AZM@GP electrode, and was employed as the anode in EAB-biosensor. Different dosages of AZM, i.e., 2 mg, 4 mg, and 8 mg, referred to as 0.25%, 0.5% and 1% AZM@GP were under examination. Results showed that EAB-biosensor was greatly benefited from appropriate dosage of AZM (0.5% AZM@GP) with reduced start-up time period, comparatively higher voltage output, more readable electrical signal and increased inhibition rate (30%-65% higher than control sensor with GP electrode) when exposing to toxic formaldehyde. This may be attributed to the fact that AZM inhibited the growth of non-EAM without much influence on the physiologic or metabolism activities of EAM under proper dosage. Further investigation of the biofilm morphology and microbial community analysis suggested that the biofilm formation was optimized with reduced thickness and enriched *Geobacter* with 0.5% AZM@GP dosage. This novel electrode is easily fabricated and equipped, and therefore would be a promising way to facilitate the practical application of EAB-sensors.

© Higher Education Press 2022

1 Introduction

To address water environment pollution which has been presenting mounting challenge for ecological balance and human health, water quality monitoring is recognized as an effective measure to guarantee water safety as it provides

real-time information online and raises alerts for incoming pollutants (Ejeian et al., 2018). Among all the environment monitoring technologies, biosensor stands out for its ability to demonstrate the biological effects of pollutants and has aroused wide attention (Antonacci and Scognamiglio, 2020, Dong et al., 2020, Yi et al., 2020). Biosensors based on electroactive biofilm (EAB) have been intensively investigated in recent two decades as it enables water quality early-warning in real-life where most pollution incidents are unpredictable, showing a comprehensive and immediate response toward many kinds of

✉ Corresponding authors

E-mail: jiangyongchange@163.com (Y. Jiang); liangpeng@tsinghua.edu.cn (P. Liang)

substances (Qi et al., 2021).

Electroactive microorganisms (EAMs) which are capable of generating and/or absorbing electrons spontaneously without additional exogenous mediator or electron shuttle, can embed in the endogenous extracellular polymeric substances (EPS) and form EAB capable of extracellular electron transport (EET) on the interface of insoluble mineral and electrode (Schröder et al., 2015; Pentassuglia et al., 2018; Logan et al., 2019). In a dual-chamber EAB-sensor, substrate is oxidized by EAB and the electron produced is transferred to electrode through direct or indirect electron transport pathway in anodic chamber. Meanwhile proton was transferred to the cathodic chamber through proton exchange membrane (PEM) or cation exchange membrane (CEM). Without specific receptor, any fluctuation of organic matter load or intrusion of toxic substance in water environment will influence the respiratory of microbes, causing sufficient change of electrical signal within a very short time (Li et al., 2020a). EAB-sensors are prospective in water quality online monitoring and quick response for its unnecessary of exogenous mediator and input energy (Shi et al., 2016). As for stability, mature EAB delivers stable electrical signal with little fluctuation. Besides, EAB-sensors use immobilized biofilm as sensing element, making it possible for the online monitoring in continuous flow compared to the luminescent bacteria in suspension form (Qi et al., 2021; Catania et al., 2021).

Recent developments have underlined the significance of increasing the sensitivity in water quality warning, which is considered a major metric for the performance of EAB-biosensors. Several efforts have been made to increase the sensitivity through regulating operation condition of EAB-biosensors by adjusting external resistance, applied potential and current, as well as by employing transient state or open circuit mode (Jiang et al., 2017; Adekunle et al., 2019). Researchers also found that optimized flow rate and reactor scale would contribute to better sensitivity of biosensor by enhancing mass transfer between the biofilm and influent (Jiang et al., 2019; Hackbarth et al., 2020). Modification of EAB and regulation on its microbial community by adding signal molecules have also been acknowledged as an effective measure to improve biosensor's performance (Ren et al., 2019; Wasito et al., 2019; Qi et al., 2020a). However, these regulation technologies are not convenient for practical engineering application and are limited to specific cases, leading to the lack of feasibility.

Antibiotics, have also been used as the agonist in several BES studies aimed at improving power generation where they were found to facilitate the enrichment of EAM and to regulate genes expression (Zhou et al., 2017; Wu et al., 2020). These findings suggest that EAB-biosensor would potentially benefit from regulated physiologic activity of EAM by antibiotics, such as promoted permeability of microbe membrane, as well as optimized biomass and

microbial community (Wen et al., 2011). Specifically, researchers have already correlated microbial community of EAB to toxicity sensitivity, for a greater abundance of *Geobacter* showed a higher sensitivity toward formaldehyde (Li et al., 2020b; Li et al., 2021). In addition, increased mass transfer efficiency on the surface of biofilm was found crucial to the toxicity sensitivity (Qi et al., 2020a). Antibiotics can regulate the biomass and thickness of EAB for its inhibition effect on microbes and may achieve the increased mass transfer. However, those antibiotics employed in previous BES studies mentioned above were soluble species, which were not applicable or eco-friendly for water environment monitoring with continuous flow of feed water. Azithromycin (AZM), a kind of insoluble antibiotics which belongs to macrolides group, establishes a major in-vitro antibacterial activity against aerobic Gram-positive cocci and Gram-negative bacillus. For its specific antibacterial spectrum, AZM may enrich the EAM by inhibiting the growth of non-EAM and regulating the physiologic or metabolism activities of EAM at a specific dosage. At the same time, the thickness of EAB may be controlled.

Therefore, with the purpose of regulating the biofilm thickness and microbial community of EAB, AZM was applied with graphite powder (GP) to form a novel AZM@GP composite electrode and to serve as the anode of EAB-biosensor. The sensitivity of the biosensor was significantly increased for water quality early-warning, with different antibiotic dosages under investigation for the effects on the sensitivity. Further determinations of the morphology and microbial community of EAB revealed how the biofilm would be affected by AZM@GP composite electrode to deliver stimulated sensing performance.

2 Materials and methods

2.1 Materials

The preparation of AZM@GP composite electrode requires the following materials: GP (99.95% metal basis, purchased from Macklin Co., Ltd., Shanghai, China), ethanol anhydrous (pharmaceutical grade, 99.95%, purchased from Macklin Co., Ltd., Shanghai, China), polytetrafluoroethylene (PTFE, 60 wt% dispersion in H₂O, purchased from Sigma-Aldrich Chemistry, USA), and AZM (dispersible tablets provided by Ouyi Pharmaceutical Co., Ltd., Shijiazhuang, China).

2.2 Preparation and operation of EAB sensor

AZM@GP composite electrode was fabricated following the methods of preparing composite activated carbon anode in an earlier study, where the activated carbon and stainless steel mesh was replaced with GP and titanium

mesh respectively (Peng et al., 2012). The preparation principle was shown in Fig. 1A. Before processing, AZM was pre-treated by ultrasonic to disperse AZM powders into ethanol anhydrous at different concentrations, i.e., 0.25%, 0.5% and 1%. Then the graphite powder (0.72 g) and PTFE solution (0.08 g) were mixed in a beaker. Ethanol anhydrous containing AZM (0.8 mL) was added dropwise into the mixture as medium to form graphite paste, followed by rolling into a film at fixed size and transferred onto a piece of titanium mesh working as current collector. After drying at room temperature for 5 min, the titanium mesh coated with graphite film was compressed at 10 MPa for another 5 min. The product was dried overnight at room temperature to remove residual ethanol. The AZM@GP electrodes were then cut into a round piece (3 cm in diameter) to fit with the silicone pad and reactor module. Depending on different dosages of AZM applied in 0.8 g GP electrodes, i.e., 2 mg, 4 mg, and 8 mg, the final products were referred to as 0.25% AZM@GP, 0.5% AZM@GP and 1% AZM@GP, respectively. Bare GP electrode was prepared as the control with pure ethanol anhydrous free of AZM and was referred to as GP. Enrofloxacin (ENR) was also tested at 0.25% (2 mg in 0.8 g GP electrode, referred to as 0.25% ENR@GP).

Dual-chamber BES reactors were constructed where the anode chamber (6 mL working volume) and cathode chamber (24 mL working volume) were divided by a cation exchange membrane (CMI7000, Membranes International Inc., USA). Prepared AZM@GP composite electrode served as the anode and carbon brush (3 cm in diameter and 3 cm in length, Sanye Carbon Co. Ltd., China) served as the cathode. Before devising, the carbon brushes were cleaned in acetone overnight and rinsed with deionized water. To monitor the output voltage, the anode and cathode were connected with an external resistance of 1000 Ω .

The reactors were cultured with mixed bacteria concentrate collected by centrifuging the effluent of a long-operated acetate-fed microbial fuel cell (MFC) at 9000 rpm for 5 min. During the startup period, the anolyte of the reactors contained 0.1 g/L CaCl₂, 0.1 g/L MgCl₂, 0.31 g/L NH₄Cl, 3.4 g/L K₂HPO₄·3H₂O, 4.4 g/L KH₂PO₄, 12.5 mL/L trace minerals, 5 mL/L vitamin solution and 1.64 g/L NaAc as the electron donor, while the catholyte contained 3.4 g/L K₂HPO₄·3H₂O, 4.4 g/L KH₂PO₄, and 16.46 g/L K₃[Fe(CN)₆]. The trace minerals solution and vitamin solution were prepared as previous studies (Cheng et al., 2009). All experiments were carried out in triplicate in batch mode at a temperature of 32°C. The voltage

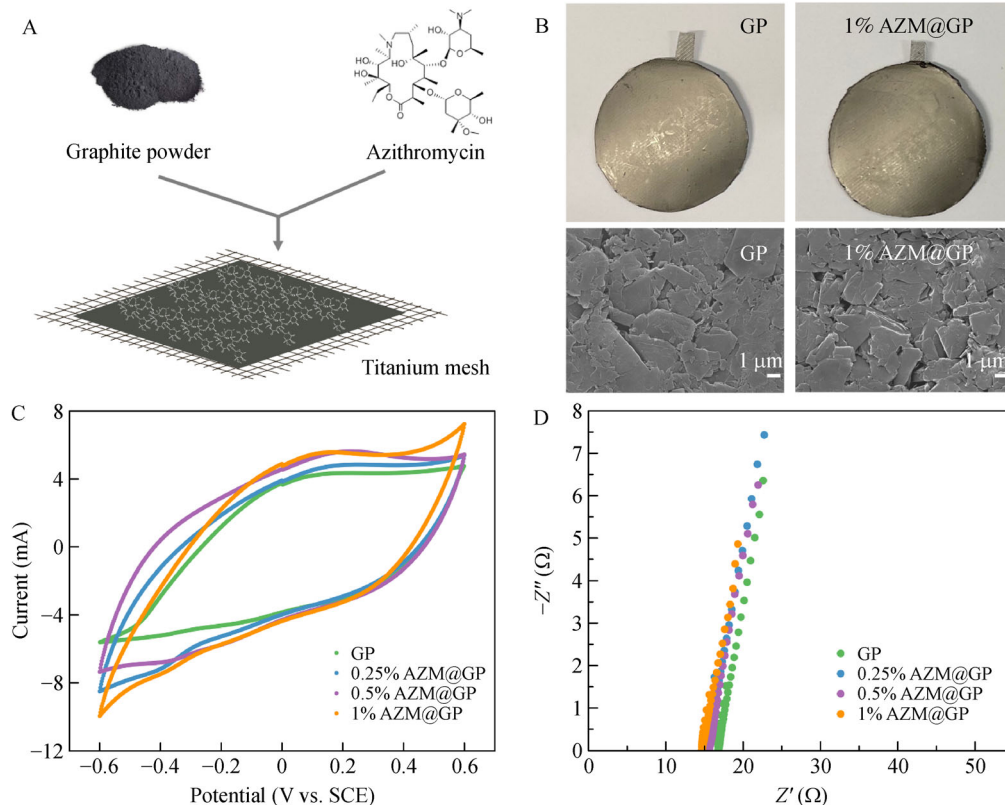


Fig. 1 (A) Preparation principle of AZM@GP, (B) true-color photographs and SEM images of GP and 1% AZM@GP electrode, (C) CV curves of GP and AZM@GP composite electrode, (D) EIS plots of GP and AZM@GP composite electrode.

produced were recorded with a data acquisition device (model 2750, Keithley Instruments, Inc.) every 30 min during start-up.

2.3 Toxicity tests and quantitative calculation of EAB-biosensor

When the reactor developed a mature biofilm to generate steady output voltage, formaldehyde was fed as the toxic substance to test the sensitivity of the biosensor. Meanwhile, the acetate concentration was reduced to 0.82 g/L and the flow rate was maintained at 2.5 mL/min to allow a hydraulic retention time of 2.4 min. The voltage signals produced were recorded every 5 s during toxicity tests. Normalized electrical signal (NES) and inhibition rate (IR) were determined as metrics for the sensitivity of EAB-biosensors and were calculated as follows (Qi et al., 2019).

$$NES = \frac{V_i}{V_0}, \quad (1)$$

$$IR = \frac{V_0 - V_n}{V_0} = \frac{\Delta V}{V_0} \times 100\%, \quad (2)$$

where V_i is the voltage during the toxicity tests with the time, V_0 is the stable voltage produced before the toxicity tests, V_n is the voltage after the toxicity tests, and ΔV is the voltage change.

2.4 Electrochemical, morphology characterization and microbial community analyses of EAB

Cyclic voltammetry (CV) was measured to characterize the electrochemical performance of the device, where a saturated calomel electrode (SCE, +242 mV vs. standard hydrogen electrode, SHE) was applied as reference electrode and inserted in the anode chamber near the prepared composite electrode. Non-turnover CV was performed under a scan rate of 0.01 V/s at a voltage range from -0.6 to 0.6 V both before and after inoculation using an electrochemical workstation (Autolab, Metrohm Co. Ltd., Switzerland).

A field-emission scanning electron microscope (SEM, JEOL JSM 6301F, Japan) was employed to observe the morphology of EAB after toxicity tests. The 3D images of EAB were obtained using the confocal laser scanning microscopy (CLSM, Leica TCS SP8, Germany) after the samples were stained with LIVE/DEAD[®] BacLight[™] Bacterial Viability Kits (Invitrogen Detection Technologies, China Branch) for 15 min. The thickness of EAB was determined according to the front view of 3D structure captured using ImageJ software (National Institutes of Health, USA).

After all the characterizations, the biofilm remaining on the electrode was scraped off for DNA extraction, PCR

amplification, and Illumina sequencing. DNA was extracted using ALFA-SEQ Advanced Soil DNA Kit (Shenzhen, China), followed by the hypervariable region V3-V4 of 16S rRNA gene going through PCR amplification by employing the universal premier 338F (5'-ACTCCTACGGGAGGCAGCAG-3') and 806 R (5'-GGACTACHVGGGTWTCTAAT-3'). The amplicons were then under sequencing on Illumina MiSeq platform (Illumina, San Diego, USA) commercially.

3 Results and discussion

3.1 Morphology and electrochemical performance of AZM@GP electrodes

The morphology of three prepared AZM@GP electrodes and GP electrode appeared similar. Taking GP and 1% AZM@GP for examples, they had a surface view alike the graphite rod presenting gray luster (Fig. 1B). Images obtained by SEM also showed a similar micro-structure for GP and 1% AZM@GP. Additional antibiotics did not cause sufficient change in electrochemical performance of GP electrode either, as revealed by CV and EIS results (Figs. 1C and 1D).

3.2 Electrical signal output during start-up

The dual-chamber EAB-biosensor was fabricated as shown in Fig. 2A. In the start-up phase, the reactors devised with AZM@GP composite electrodes took around 27 days to deliver reproducible output voltages, a much-reduced time period as compared to that required by the reactor with GP electrode (35 days) (Fig. 2B). It is noticeable that graphite electrode employed in all the devices may be a major contributor for the comparatively long startup time period as it has a homogeneous surface that is extremely smooth and glossy and is hard for microbes to adhere (Pentassuglia et al., 2018). However, GP delivers much lower capacitance than activated carbon and thus is considered more adapted for serving as the electrode of a biosensor. In addition to shortening the startup, the voltage output was significantly increased with AZM in the electrode, where the maximum voltage of 512 mV was produced by the biosensor with 0.5% AZM@GP electrode, 23% higher than that of GP (415 mV) (Fig. 2B). This result was in line with an earlier finding that current density output of BES device would be improved when adding 0.5 and 0.1 mg/L tobramycin into the electrolyte, which can be ascribed to the positive contribution of antibiotics on EAB formation and performance under subminimal inhibitory concentrations (sub-MIC) (Zhou et al., 2017). At a low concentration in the composite electrode (under 0.5%), AZM mainly inhibited the growth of non-EAM without much influence on the physiologic

activities of EAM, as evidenced by high voltage output then. By inhibiting the biological activity of Gram-positive bacteria, EAMs which mostly belong to Gram-negative bacillus may have access to more organic matters per unit mass to generate electricity. Some other studies also found enhanced power generation in MFC with the presence of antibiotics and revealed that the cells exposed to sub-MIC of antibiotics presented a crucial upregulation in the expression of c-type cytochrome genes that was closely related with intercellular electron transfer in *Geobacter* and long-distance electron transfer in EABs, leading to enhanced electrochemical activity of EAB (Reguera et al., 2005; Summers et al., 2010; Zhou et al., 2017). However, the biosensor with 1% AZM@GP electrode delivered much reduced voltage output of 88 mV than those with less AZM dosages, suggesting an inhibited electrochemical performance of EAB. A possible explanation is that AZM over specific bactericidal concentration would inhibit bacterial growth by blocking the activity of peptide acyltransferase in the ribosome and consequently stopping the synthesis of protein. Increasing capacitance was found in CV curves after inoculation for all tested electrodes, evidencing the successive formation of EAB (Fig. S1). It was concluded that 0.25% and 0.5% AZM@GP electrode greatly reduced start-up and promoted the electrochemical activity of EAB to a parallel extent while 1% AZM@GP showed an obvious suppression.

3.3 Toxicity tests

After start-up, the formaldehyde at different concentrations was fed into the biosensor for toxicity tests. At first, the concentration of NaAc in continuous flow was 0.82 g/L to eliminate the effects of organic matters oversaturation. Once the voltage output was stabilized for 30 min, the biosensors were fed with different concentrations of formaldehyde, i.e. 0.01%, 0.02% and 0.03%. In this research, the organic content was assumed to be saturated for the formation of EAB, thus formaldehyde added can be regarded as a respiratory inhibitory effect on bacteria by decreasing the EPS and biomass as well as separating microbes from the mature biofilm (Li et al., 2020a). The voltage output during toxicity test was shown in Figure S2. By applying Eq. (1), these voltages were normalized into NES for comparison (Fig. 3). With increased formaldehyde concentration, the response time of electrical signal was greatly reduced (Figs. 3A-3C). More readable NES signal decline was observed with 0.5% AZM@GP at each tested formaldehyde concentration, suggesting a greatly increased sensitivity. However, the biosensor with 1% AZM@GP was the least sensitive when exposing to the formaldehyde among all tested biosensors, even compared with the bare GP electrode. This may be ascribed to the extremely low voltage output which 1% AZM@GP delivered. Since most EAMs were inhibited, the

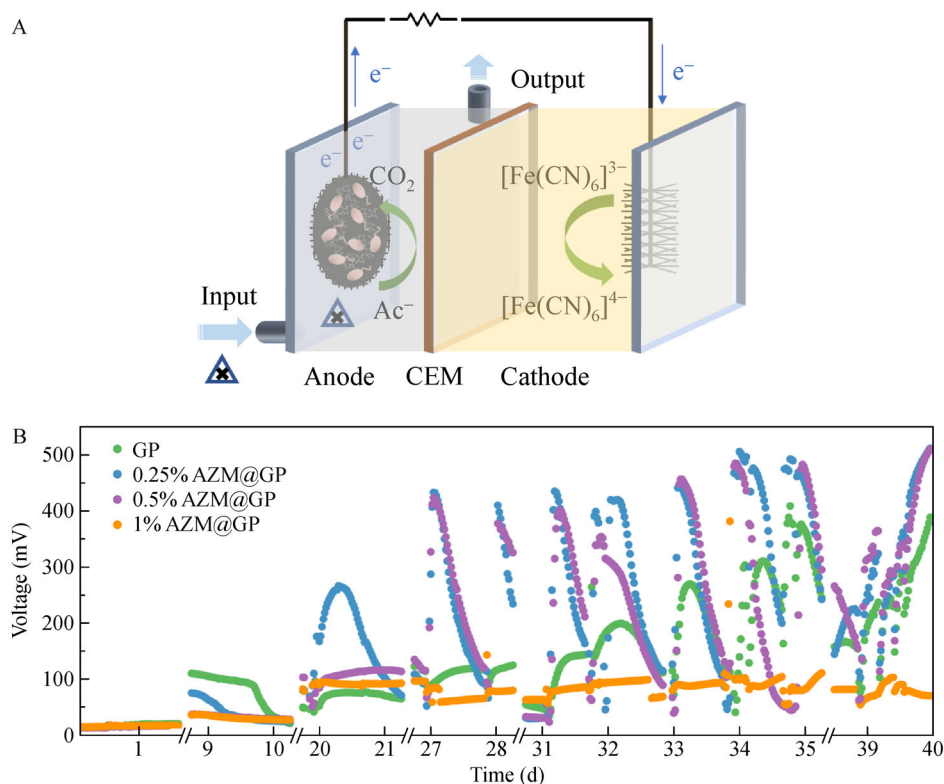


Fig. 2 (A) Schematic diagram of the built EAB-sensor, (B) Electrical signal output during start-up.

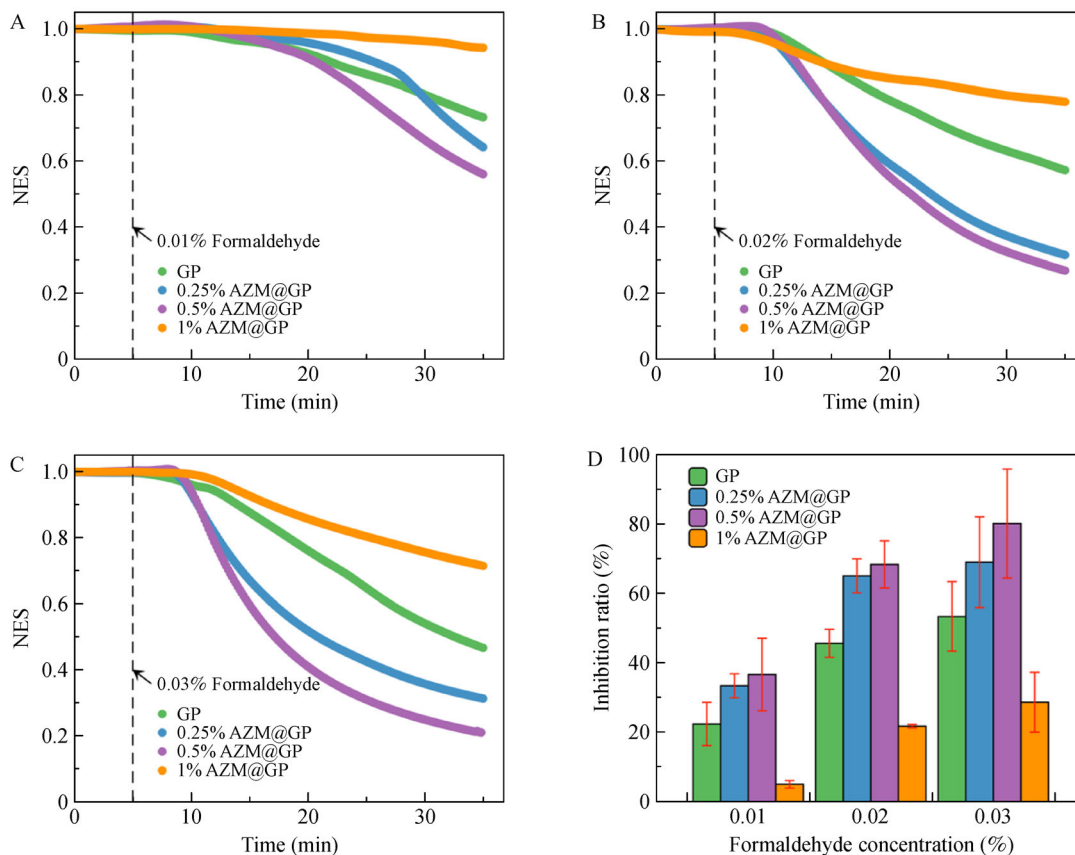


Fig. 3 Toxicity tests of formaldehyde under different concentrations. NES changes within 30 min under 0.01% (A), 0.02% (B), 0.03% (C) formaldehyde, respectively and (D) corresponding inhibition rates at 30 min.

bio-anode was less capable or incapable of sensing the toxicity introduced.

Inhibition rates calculated 30 min after feeding the formaldehyde were shown in Fig. 3D. Similar to NES results, the biosensor with 0.5% AZM@GP delivered the highest IR with each tested formaldehyde concentration, followed by the biosensor with 0.25% AZM@GP. Compared to the control biosensor devised with GP electrode, 0.5% AZM@GP would significantly improve the IR by 30% ~ 65%, depending on the formaldehyde concentration applied. It was also clear that higher formaldehyde concentration would lead to increased IR regardless of the electrode employed, evidencing the toxicity of added formaldehyde. Among the previous studies using bioanode with mixture inoculation as sensing element, the lowest responding limit varies from 0.013% to 1% and the inhibition rate varies from 0.015% to 14.6% respectively (Yu et al., 2017; Lu et al., 2019). It is obvious that this study achieved much increased sensitivity. The NES results showed earlier that the biosensor's sensitivity was greatly restrained when large amount of AZM was applied in the electrode (1% AZM@GP). This was evidenced again by IR results where the biosensor with 1% AZM@GP was found to deliver the lowest IR at each tested formaldehyde concentration.

After toxicity tests, the anolyte was extracted immediately using a syringe and the anode chamber was refilled with fresh medium containing 1.62 g/L NaAc in continuous mode. During this recovery period, NES signals rose gradually (Figure S3). It took around 130 min for EABs fed with 0.01% formaldehyde to recover, with a recovery rate among 80% and 100%. Larger formaldehyde concentration of 0.02% led to much increased recovery time to around 400 min and recovery rate reached 90% at 500 min. However, when formaldehyde concentration further increased to 0.03%, the EABs could hardly deliver well recovered NES signals and recovery ratio was lower than 80%. It showed a rough warning range of this kind of AZM@GP biosensor.

ENR which belongs to fluoroquinolone group and serves as veterinary medicine for respiratory system, digestive system and genitourinary system infections in livestock was also tested for its availability to serve in biosensor's electrode (Attili et al., 2016). Similar to the processing of AZM@GP electrode as previously described, ENR@GP electrode was prepared and referred to as 0.25% ENR@GP. The monitored voltage output of biosensor with ENR@GP was extremely low (Fig. S4A). Researchers have noticed that ENR shows a broad antibacterial effect both on Gram-positive and Gram-

negative bacillus, thus may greatly inhibit the growth of most EAM which belongs to Gram-negative bacillus group, leading to a poor electrical signal produced (Souza et al., 2004; Tarushi et al., 2010). When challenged with 0.02% formaldehyde, it also showed a relatively low response (Figure S4B). It could be concluded that not all antibiotics are suitable to serve in the electrode of a biosensor to improve sensitivity, but AZM is. Among various antibiotics, those insoluble in water and capable of inhibiting the growth of non-EAM without much influence on EAM would be applicable in EAB-sensor tested in this study.

3.4 Morphological assessments of EAB

After toxicity tests, CLSM was used to examine the 3D structure and thickness of EABs with different dosages of AZM. Green areas indicated the total biomass including living and dead cells (Figure S5 and Fig. 4A). The 3D structure presented a dense topography and the thickness differences can be easily observed. The average thickness of EABs were determined by ImageJ software. Compared with the thickness of EAB formed on GP electrode (24.05 μm), a small amount of additional AZM on GP electrode (0.25% AZM@GP) significantly increased the EAB's thickness (45.24 μm) by 88% (Fig. 4B). This finding was in accordance with a previous report that low concentration of tobramycin (0.5 mg/L in electrolyte) facilitated the formation of EAB in a BES (Zhou et al., 2017). However, when the dosage of AZM increased to 0.5% and 1%, a sudden decrease of the EAB's thickness

was observed following 0.25%, which was attributed to the enhanced antibiotic activity over the dosage of 0.5% AZM against the microbial community in EABs, preventing microbes from adhering to the plate electrode. This finding also explained why the sensitivity of EAB with 0.5% AZM@GP electrode was better than that with 0.25% AZM@GP as it was already revealed that reduced biofilm thickness was beneficial for improved sensitivity toward toxicity (Qi et al., 2020a). It can also illustrate that why 1% AZM@GP has the least sensitivity for it has merely microorganisms attached to the electrode for the great in-vitro effect of antibiotics.

The morphology of four obtained EABs observed by SEM showed sufficient differences (Fig. 4C). The EAB on GP electrode was composed of uniform microbes which were all gathered together and wrapped thoroughly in EPS. While the EABs on 0.25% AZM@GP and 0.5% AZM@GP electrodes exhibited a less dense pattern consisting several gaps between microbes loosely distributed. The morphology of EAB on 1% AZM@GP electrode was totally distinct from the others as it was consisted of many rod-shaped bacteria clusters, suggesting that the EPS content was further reduced, leading to the stack of individual bacteria under over high dosage of antibiotics.

3.5 Microbial community analysis

The functions of EAB were closely in accordance with microbial community structure, ranging from organic matters metabolism, electron transfer to toxicity resistance

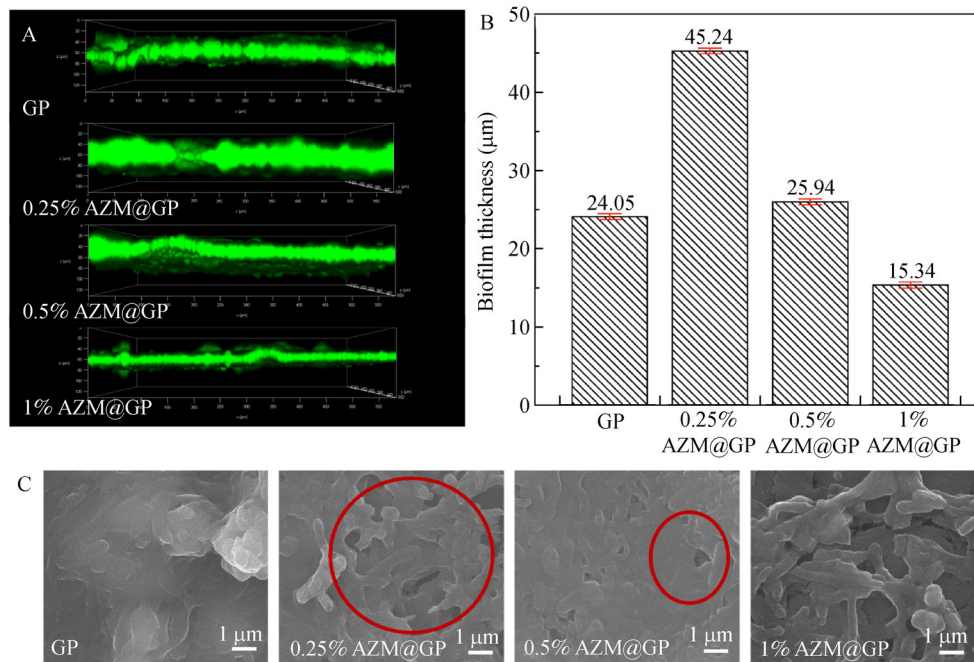


Fig. 4 (A) Front view of CLSM images, (B) calculated biofilm thickness, (C) SEM images of EABs formed on different electrodes.

(Pan et al., 2020). As for the α -diversity statistics, to explore the impact of introduced antibiotics on microbial species richness, Chao 1 indicator was employed calculated and determined by applying the number of rare species that would be found when a community was being sampled to estimate the likelihood of undiscovered species existed. Thus, Chao 1 indicator has nothing to do with species abundance and evenness, but is particularly sensitive to rare species. The richness of a community decreases as the indicator decreases, as it shows in Fig. 5A.

It was found that the species richness of EAB decreased with more AZM added in GP electrode until it exceeded 0.5%, from 180.2 to 131.9, which may be attributed to the antibiotic effect of AZM on Gram-positive bacteria. Further increasing AZM dosage to 1%, Chao 1 indicator showed a sharp rise, suggesting that 1% was higher than the dosage threshold of AZM to *Geobacter*. Also seen in Fig. 5B, the relative abundance of the *Geobacter* declined while the increases of other bacteria were observed. The reduction of predominant species may provide more

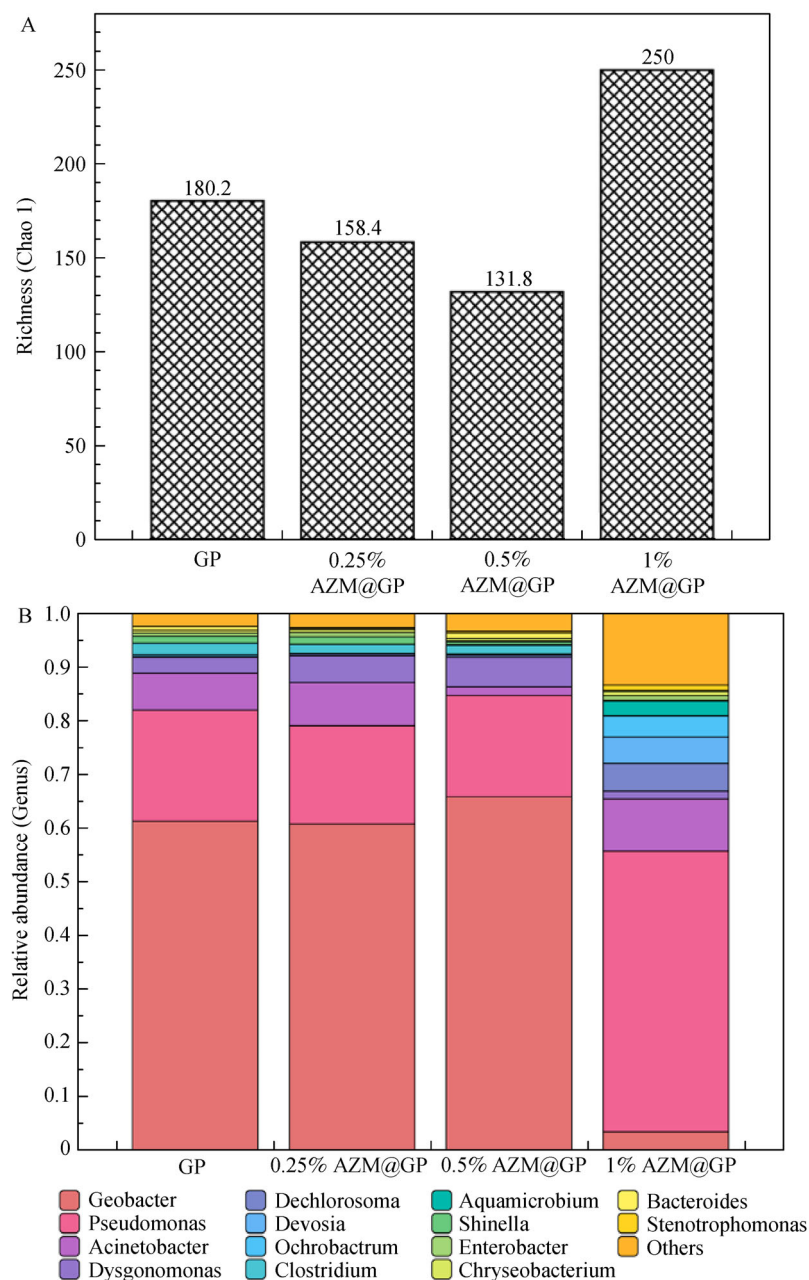


Fig. 5 Microbial community analyses of EABs. (A) Chao 1 indicator, (B) relative abundance of microbial community.

organic matters and lead to the development of other rare species. The Chao 1 indicator demonstrated that the introduction of AZM under specific dosage promoted interspecific homogeneity at a sacrifice of there being fewer species (Sui et al., 2021).

Results obtained from microbial community analysis revealed that the relative abundance of *Geobacter* in EABs slight increased from 61% to 66% after the GP electrode modified with 0.5% AZM@GP (Fig. 5B). This may be the result of the antibiotic spectrum of AZM which would first inhibit the growth of gram-positive bacteria, basically non-EAMs, leading to the rise of relative abundance of EAMs. Given that biosensor's electrical signals are mostly produced by EAMs and that EAMs suppressed by toxicity intrusion greatly contribute to signal drop, enriched *Geobacter* in EAB would facilitate the utilization of organic matters and the generation of electricity, leading to a more readable output electrical signal toward toxic substances (Lovley, 2008). This was in line with the previous study, where low concentration of sodium acetate would facilitate the enrichment of *Geobacter* and therefore increase the toxicity sensitivity of formaldehyde (Li et al., 2021).

4 Conclusions

This study employed additional antibiotics, AZM, with graphite powder to form AZM@GP composite electrode, which served as the anode in EAB-biosensor for improved sensitivity. Among different tested dosages of AZM in the composite electrode, 0.5% AZM was found advantageous to devise a biosensor as it enabled much reduced start-up time and increased sensitivity toward formaldehyde. Investigations of biofilm morphology and microbial community suggested that this result could be ascribed to the decreased thickness of EAB and the relatively high abundance of *Geobacter* under the regulation of antibiotics by excluding the unwanted population in anode. The sensitivity of this system toward other toxic substrates remains to be studied before the composite electrode will be used in actual water quality warning in the future.

Acknowledgements This work was supported by the National Natural Science Foundation of China (Grant No. 52125001).

Electronic Supplementary Material Supplementary material is available in the online version of this article at <https://doi.org/10.1007/s11783-022-1518-7> and is accessible for authorized users.

References

Adekunle A, Raghavan V, Tartakovsky B (2019). On-line monitoring of heavy metals-related toxicity with a microbial fuel cell biosensor. *Biosensors & Bioelectronics*, 132: 382–390

Antonacci A, Scognamiglio V (2020). Biotechnological advances in the

design of algae-based biosensors. *Trends in Biotechnology*, 38(3): 334–347

Attili A R, Prezioso S, Ngu Ngwa V, Cantalamessa A, Moriconi M, Cuteri V (2016). Clinical evaluation of the use of enrofloxacin against *Staphylococcus aureus* clinical mastitis in sheep. *Small Ruminant Research*, 136: 72–77

Catania C, Karbelkar A A, Furst A L (2021). Engineering the interface between electroactive bacteria and electrodes. *Joule*, 5(4): 743–747

Cheng S, Xing D, Call D F, Logan B E (2009). Direct biological conversion of electrical current into methane by electromethanogenesis. *Environmental Science & Technology*, 43(10): 3953–3958

Dong S, Yin C, Chen X (2020). Toxicity-oriented water quality engineering. *Frontiers of Environmental Science & Engineering*, 14(5): 80

Ejeian F, Etedali P, Mansouri-Tehrani H A, Soozanipour A, Low Z X, Asadnia M, Taheri-Kafrani A, Razmjou A (2018). Biosensors for wastewater monitoring: A review. *Biosensors & Bioelectronics*, 118: 66–79

Hackbarth M, Jung T, Reiner J E, Gescher J, Horn H, Hille-Reichel A, Wagner M (2020). Monitoring and quantification of bioelectrochemical *Kyrpidia spormannii* biofilm development in a novel flow cell setup. *Chemical Engineering Journal*, 390: 124604

Jiang Y, Chu N, Zeng R J (2019). Submersible probe type microbial electrochemical sensor for volatile fatty acids monitoring in the anaerobic digestion process. *Journal of Cleaner Production*, 232: 1371–1378

Jiang Y, Liang P, Liu P, Miao B, Bian Y, Zhang H, Huang X (2017). Enhancement of the sensitivity of a microbial fuel cell sensor by transient-state operation. *Environmental Science. Water Research & Technology*, 3(3): 472–479

Li T, Chen F, Zhou Q, Wang X, Liao C, Zhou L, Wan L, An J, Wan Y, Li N (2020a). Unignorable toxicity of formaldehyde on electroactive bacteria in bioelectrochemical systems. *Environmental Research*, 183: 109143

Li T, Liao C, An J, Zhou L, Tian L, Zhou Q, Li N, Wang X (2021). A highly sensitive bioelectrochemical toxicity sensor and its evaluation using immediate current attenuation. *Science of the Total Environment*, 766: 142646

Li T, Zhou Q, Zhou L, Yan Y, Liao C, Wan L, An J, Li N, Wang X (2020b). Acetate limitation selects *Geobacter* from mixed inoculum and reduces polysaccharide in electroactive biofilm. *Water Research*, 177: 115776

Lu H, Yu Y, Zhou Y, Xing F (2019). A quantitative evaluation method for wastewater toxicity based on a microbial fuel cell. *Ecotoxicology and Environmental Safety*, 183(2019): 109589

Logan B E, Rossi R, Ragab A, Saikaly P E (2019). Electroactive microorganisms in bioelectrochemical systems. *Nature Reviews. Microbiology*, 17(5): 307–319

Lovley D R (2008). The microbe electric: Conversion of organic matter to electricity. *Current Opinion in Biotechnology*, 19(6): 564–571

Pan J, Hu J, Liu B, Li J, Wang D, Bu C, Wang X, Xiao K, Liang S, Yang J, Hou H (2020). Enhanced quorum sensing of anode biofilm for better sensing linearity and recovery capability of microbial fuel cell toxicity sensor. *Environmental Research*, 181: 108906

Peng X, Yu H, Wang X, Zhou Q, Zhang S, Geng L, Sun J, Cai Z (2012). Enhanced performance and capacitance behavior of anode by rolling

- Fe₃O₄ into activated carbon in microbial fuel cells. *Bioresource Technology*, 121: 450–453
- Pentassuglia S, Agostino V, Tommasi T (2018). *Encyclopedia of Interfacial Chemistry*. Wandelt, K. (ed). Oxford: Elsevier, 110–123
- Qi X, Liu P, Liang P, Hao W, Li M, Huang X (2019). Dual-signal-biosensor based on luminescent bacteria biofilm for real-time online alert of Cu(II) shock. *Biosensors & Bioelectronics*, 142: 111500
- Qi X, Liu P, Liang P, Hao W, Li M, Li Q, Zhou Y, Huang X (2020a). Biofilm's morphology design for high sensitivity of bioelectrochemical sensor: An experimental and modeling study. *Science of the Total Environment*, 729: 138908
- Qi X, Wang S, Li T, Wang X, Jiang Y, Zhou Y, Zhou X, Huang X, Liang P (2021). An electroactive biofilm-based biosensor for water safety: Pollutants detection and early-warning. *Biosensors & Bioelectronics*, 173: 112822
- Reguera G, McCarthy K D, Mehta T, Nicoll J S, Tuominen M T, Lovley D R (2005). Extracellular electron transfer via microbial nanowires. *Nature*, 435(7045): 1098–1101
- Ren L, McCuskey S R, Moreland A, Bazan G C, Nguyen T Q (2019). Tuning *Geobacter sulfurreducens* biofilm with conjugated polyelectrolyte for increased performance in bioelectrochemical system. *Biosensors & Bioelectronics*, 144: 111630
- Schröder U, Harnisch F, Angenent L T (2015). Microbial electrochemistry and technology: Terminology and classification. *Energy & Environmental Science*, 8(2): 513–519
- Shi L, Dong H, Reguera G, Beyenal H, Lu A, Liu J, Yu H Q, Fredrickson J K (2016). Extracellular electron transfer mechanisms between microorganisms and minerals. *Nature Reviews. Microbiology*, 14 (10): 651–662
- Souza M J E, Bittencourt C F, Filho P D S E S (2004). Microbiological assay for enrofloxacin injection. *International Journal of Pharmaceutics*, 271(1): 287–291
- Sui M, Li Y, Jiang Y, Zhang Y, Wang L, Zhang W, Wang X (2021). Light exposure interferes with electroactive biofilm enrichment and reduces extracellular electron transfer efficiency. *Water Research*, 188: 116512
- Summers Z M, Fogarty H E, Leang C, Franks A E, Malvankar N S, Lovley D R (2010). Direct exchange of electrons within aggregates of an evolved syntrophic coculture of anaerobic bacteria. *Science*, 330 (6009): 1413–1415
- Tarushi A, Raptopoulou C P, Psycharis V, Terzis A, Psomas G, Kessissoglou D P (2010). Zinc(II) complexes of the second-generation quinolone antibacterial drug enrofloxacin: Structure and DNA or albumin interaction. *Bioorganic & Medicinal Chemistry*, 18 (7): 2678–2685
- Wasito H, Fatoni A, Hermawan D, Susilowati S S (2019). Immobilized bacterial biosensor for rapid and effective monitoring of acute toxicity in water. *Ecotoxicology and Environmental Safety*, 170: 205–209
- Wen Q, Kong F, Zheng H, Cao D, Ren Y, Yin J (2011). Electricity generation from synthetic penicillin wastewater in an air-cathode single chamber microbial fuel cell. *Chemical Engineering Journal*, 168(2): 572–576
- Wu D, Sun F, Chua F J D, Zhou Y (2020). Enhanced power generation in microbial fuel cell by an agonist of electroactive biofilm–Sulfamethoxazole. *Chemical Engineering Journal*, 384: 123238
- Yi X, Gao Z, Liu L, Zhu Q, Hu G, Zhou X (2020). Acute toxicity assessment of drinking water source with luminescent bacteria: Impact of environmental conditions and a case study in Luoma Lake, East China. *Frontiers of Environmental Science & Engineering*, 14 (6): 109
- Yu D, Zhai J, Liu C, Zhang X, Bai L, Wang Y, Dong S (2017). Small microbial three-electrode cell based biosensor for online detection of acute water toxicity. *ACS Sensors*, 2(11): 1637–1643
- Zhou L, Li T, An J, Liao C, Li N, Wang X (2017). Subminimal inhibitory concentration (sub-MIC) of antibiotic induces electroactive biofilm formation in bioelectrochemical systems. *Water Research*, 125: 280–287